2024 International Conference on Quantum Communications, Networking, and Computing (QCNC) | 979-8-3503-6677-8/24/$31.00 ©2024 IEEE | DOI: 10.1109/QCNC62729.2024.00011

# Quantum Transduction Models for Multipartite Entanglement Distribution

Laura d'Avossa, Angela Sara Cacciapuoti, *Senior Member, IEEE*, Marcello Caleffi, *Senior Member, IEEE*

***Abstract*—Multipartite entanglement distribution is a key functionality of the Quantum Internet. In this paper, the multipartite entanglement distribution is analyzed from a quantum transduction perspective. Specifically, communication models for quantum transduction of multipartite entangled states are provided, and they rely on a different paradigms, resulting from the capabilities of different hardware platforms underlying quantum transduction. By using terminology and concepts tailored for the communications engineering community, the objective of the paper is to depart from the large heterogeneity of hardware solutions available in literature, in order to abstract from the particulars of the specific solution.**

***Index Terms*—Quantum Internet, Quantum Transduction, Entanglement distribution, Multipartite entanglement, Teleporting.**

## I. Introduction

The Quantum Internet is envisioned to rely on hybridisation of network architectures and technologies to face with the compulsory challenges connected to its design [1]. Indeed, several technologies are available to store, process, transmit quantum bit (qubits). And each qubit physical implementation has its own set of pros and cons [1].

*Superconducting technology* is recognized as a very promising quantum computing platform due to its capabilities to realize fast gates and due to its high scalability. However, the superconducting technology requires cryogenic temperatures, which in turn challenge the development of large-scale quantum networks. On the other hand, *photonic technology* is worldwide recognized as the most suitable technology for realizing the so-called *flying qubits*, i.e., optical photons acting as quantum carriers, which travel along communication channels for fulfilling quantum communication needs. And, indeed, optical photons weakly interact with the environment (thus, less subjected to decoherence), can be easily controlled with standard optical components as well as are characterized by high-rate low-loss transmissions [1], [2].

Due to their complementary features, superconducting and photonic technologies are envisioned to play a key role in the deployment of the Quantum Internet, where the aim of the flying qubits is to enable communications among the network nodes, by "transporting" qubits out of the physical quantum devices through the network for conveying quantum information and/or entanglement from the sender to the receiver. Hence, a quantum transducer is needed to convert a superconducting qubit within a quantum network node into a flying qubit [3]–[7].

However, flying qubits at optical frequencies (typically about hundred of THz) cannot directly interact with superconducting qubits that, differently, work at microwave frequencies (GHz). Hence, the challenges arising in designing a microwave-optical transducer are not trivial. And indeed, nowadays, it is still an open-problem to mediate the huge frequency gap – about five orders of magnitude – between microwave and optical photons.

In this paper, we provide communication models for quantum transduction based on different paradigms, resulting from the capabilities of different hardware platforms underlying quantum transduction. By using terminology and concepts tailored for the communications engineering community, the objective of the paper is to depart from the large hardware solutions available in literature, in order to abstract from the particulars of the specific solutions.

We provide such models for a key functionality of quantum communication networks, i.e., entanglement distribution. Specifically, the transduction process is investigated for mapping the entanglement between superconducting qubits into the entanglement of optical photons and vice-versa, in order to make the entanglement distribution possible.

In this context, the main contribution of the paper is modeling trasducers for the distribution of multipartite entanglement, which recently has been recognized as a crucial resource for enabling astonishing functionalities in the Quantum Internet [8]–[10].

In fact, although multipartite entanglement distribution has been analyzed from a protocol point of view [9], [11], what is missing is a consolidated literature that treats multipartite entanglement distribution with an outlook on quantum transduction.

Although the analysis we present does not have the ambition of being exhaustive, it has the merit of providing some guidelines from a communication engineering perspective.

It is worthwhile to note that one of the reason for which our modelling is far from being exhaustive is that the hardware choices influence hugely the theoretical framework. And indeed there is not a single hardware solution individuated in literature, nor a clear understanding (and analysis) of the role played by different hardware setups.

The authors are with the www.QuantumInternet.it research group, *FLY: Future Communications Laboratory*, University of Naples Federico II, Naples, 80125 Italy. A.S. Cacciapuoti and M. Caleffi are also with the Laboratorio Nazionale di Comunicazioni Multimediali, National Inter-University Consortium for Telecommunications (CNIT), Naples, 80126, Italy.

Angela Sara Cacciapuoti acknowledges PNRR MUR NQSTI-PE00000023, Marcello Caleffi acknowledges PNRR MUR project RESTART-PE00000001.

979-8-3503-6677-8/24/$31.00 ©2024 IEEE
DOI 10.1109/QCNC62729.2024.00011

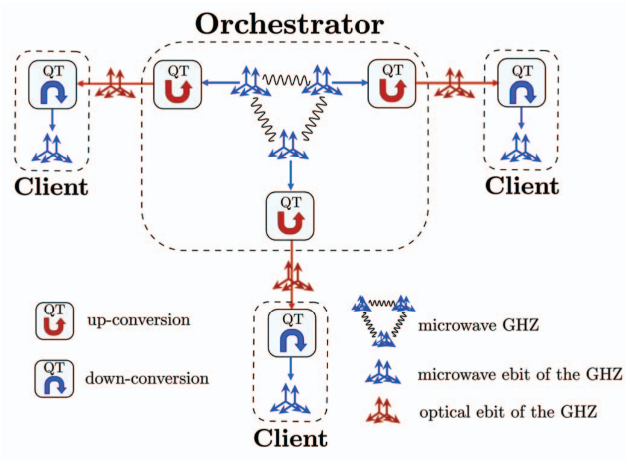


Fig. 1: DMD: *Direct Multipartite entanglement Distribution* for a 3-qubit GHZ state. This state, generated at the orchestrator, must be distributed among the three superconducting clients via optical quantum channels. Ebits at microwave and optical frequencies are depicted in blue and red, respectively. The Quantum Transducers (QTs) at the orchestrator realize an up-conversion of the ebits of the GHZ state, by converting them from microwave to optical frequencies. After being distributed through optical channels, the ebits are converted again into microwave frequencies with a down-conversion process implemented by the QTs at the clients.

We do hope that this paper will strike up a dialogue among the different research communities involved to converge on a standard reference model, which would be of paramount importance for quantum network development.

The remaining part of the paper is organised as follows. In Section II we describe the problem statement by presenting two main techniques for multipartite entanglement distribution. In Section III, we provide two different communication models for quantum transduction based on different paradigms, relying on different hardware capabilities. In Section IV, we analyze the impact of the noise on the developed models and, finally, in Section V we conclude the paper.

## II. Problem Statement: Direct vs Teleported Multipartite Entanglement Distribution

Generating and distributing entanglement constitutes a demanding task due to the delicate nature of quantum states and their susceptibility to environmental disturbances. The complexity of entanglement generation and distribution becomes even more evident when it comes to multipartite entangled states, such as GHZ states[1].

Indeed, the generation of multipartite entanglement requires sophisticated and resource-intensive setups, often involving complex experimental apparatuses and precise control mechanisms. This makes pragmatic to assume a specialized super-node, in the following referred to as *orchestrator*, responsible for the entanglement generation and distribution. The orchestrator is connected via quantum channels to network nodes with lower capabilities of satisfying entanglement technological and hardware requirements, referred to as *clients*. Accordingly, to eventually distribute a multipartite entangled state among the clients, the orchestrator first locally generates the multipartite entanglement state. Then, the entangled qubits – *ebits* in the following – of the multipartite state are distributed to the clients according to a chosen distribution strategy [10].

It is a matter of fact that distributing multipartite entangled states among remote superconducting quantum nodes forces the adopted distribution strategy to account for the huge frequency gap between intra- and inter-nodes frequencies, namely, between microwave and optical frequencies, by exploiting quantum transduction.

In this context, we can distinguish two main classes of multipartite entanglement distribution techniques:

i) DMD: Direct Multipartite entanglement Distribution;
ii) TMD: Teleported Multipartite entanglement Distribution.

In DMD, as suggested by the name, the ebits are directly converted from microwave to optical frequencies and vice-versa, in order to be distributed from the orchestrator to the clients. Conversely, in TMD, the ebits are teleported to the clients, once additional EPR pairs have been generated and shared between orchestrator and the clients.

### A. DMD: Direct Multipartite entanglement Distribution

Each ebit of the multipartite state can, in principle, be directly distributed to a client. This task requires to perform two different frequency conversions for each ebit of the multipartite entangled state:

- *up-conversion*: this process converts an ebit from microwave to optical frequencies, i.e., it converts a microwave ebit-carrier into a optical ebit-carrier,
- *down-conversion*: this process enables the inverse conversion, i.e., it converts an ebit from optical to microwave frequencies.

Once this twofold up- and down conversion process is completed for each client, the multipartite entangled state has been distributed among all the nodes, as schematized in Fig. 1.

It is important to highlight that both up- and down-conversion processes are not deterministic. Indeed, there exists

[1] A Greenberger–Horne–Zeilinger (GHZ) state – formally, $|GHZ\rangle = \frac{|0\rangle^{\otimes n} + |1\rangle^{\otimes n}}{\sqrt{2}}$ for $n$-qubit state [13] – is a maximally entangled state, characterised by maximally *connectivity*. Indeed, a state is maximally connected if, for any two qubits, there exists a sequence of single-qubit measurements on the remaining qubits that, when performed, guarantee that the two qubits end up in a maximally entangled state [14]. On the other hand, GHZ states exhibit minimum *persistency*, i.e., equal to 1. Indeed the persistency of a multipartite entangled state is the minimum number of qubits that need to be measured to guarantee that the resulting state is unentangled [9], [14].

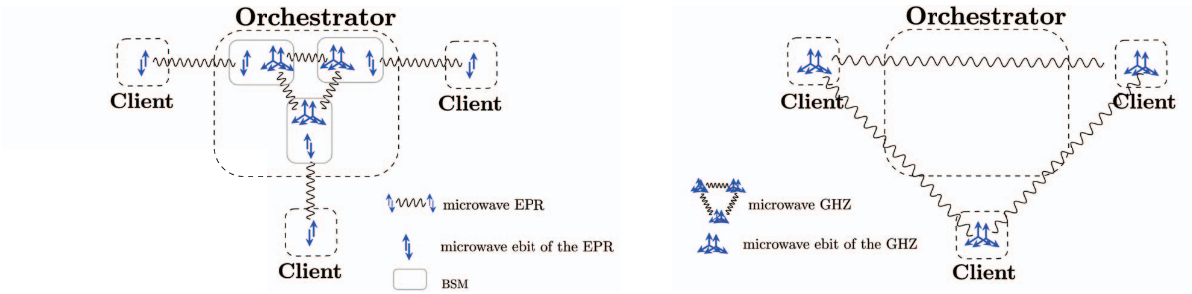


(a) Network state before the teleportation process: the multipartite state is stored at the orchestrator, and EPR pairs have been generated and distributed (ideally) so that one microwave ebit is at the orchestrator and the other microwave ebit is at each client.

(b) Network state after the teleportation process: by consuming the EPR pairs during the teleportation processes, each microwave ebit of the multipartite state – a 3-qubit GHZ state in this case – is teleported at the corresponding client.

Fig. 2: TMD: *Teleported Multipartite entanglement Distribution* for the same multipartite state considered in Fig 1. First, the orchestrator generates and share three EPR pairs with the clients, which represents the communication resource – namely, the *artificial quantum link* [9] – utilized for teleporting the multipartite state to the clients. Then, by performing local operations – i.e., Bell State Measurements (BSMs) – between the ebits of the EPR pairs at the orchestrator and the ebits of the GHZ state, followed by classical communications [12], the 3-qubit GHZ is shared between 3 clients.

a non-zero probability that either or both the conversions fail [15]–[17], with failure-probability values strictly depending on the characteristics of hardware used for implementing the microwave-optical transduction. Quantum transducer exhibits successful bi-directional (i.e., microwave to optical or vice-versa) conversion probability (also defined as *total efficiency*) in the order of $10^{-2}$ [5], [18]. Indeed, despite big efforts in the realization of quantum transducers, obtaining high efficiency is still an open and crucial challenge [19]. Furthermore, a successful DMD requires to preserve the multipartite state, originally generated at the orchestrator, during the distribution process. This implies that each ebit must be preserved during both up- and down-conversion processes (as well as during the carrier propagation process through the optical link) for each client. Clearly, if all the aforementioned processes succeed, the original multipartite state is preserved. Conversely, whether at least one of the processes for any client fails, then the preservation of the entire multipartite state is compromised. And if the entanglement among the remaining (un-failed processes) ebits can be preserved, it is not assured, since it depends on the specific class of multipartite entangled state to be distributed. Indeed, the DMD approach is not viable for all the classes of multipartite entanglement, which are characterized by different *persistence* properties [14]. As an example, the direct distribution of GHZ-like states, which are characterized by the lowest persistence, requires all the photons encoding the GHZ state to be successfully distributed to the clients in a single distribution attempt [11], [20], [21]. Hence, even the loss of a single ebit of the original GHZ state – during the conversions or the transmission through the optical channel – results in the disruption of the whole multipartite state.

### B. TMD: Teleported Multipartite entanglement Distribution

Differently from DMD, TMD exploits the preliminary distribution of EPR pairs to the clients to eventually distribute the multipartite entangled state via quantum teleporting protocol. Specifically, once multiple[2] (one for each client) EPR pairs have been generated, the orchestrator retains one ebit of each EPR pair while distributing the others to the clients. Once the EPR distribution process is completed, the original multipartite entangled state is teleported at the clients by performing local operations and classical communications [1], as depicted in Fig. 2.

According to the above description, TMD shifts the impact of noisy quantum transduction (and noisy optical ebit carrier propagation) from multipartite entanglement state to EPR pairs. In other words – and differently from DMD – in TMD quantum transduction acts on EPR pairs only and no up- or down-conversion of the multipartite ebits is required. Indeed EPR pairs generation and distribution is less demanding than multipartite entanglement generation and distribution. Notably, this shift makes TMD strategy viable for all the classes of multipartite entanglement, regardless of their persistence properties. Moreover, TMD strategy guarantees more resilience to noise and better protection against memory decoherence [20], [22].

For all these reasons, in the remaining part of the paper we focus on TMD only, by providing different communication models for quantum transduction in TMD and by discussing the different impact of noise on them.

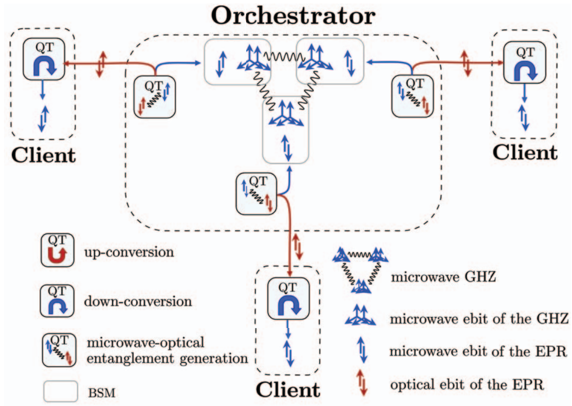


Fig. 3: TMD with plain clients: *Teleported Multipartite entanglement Distribution* with plain clients for the same multipartite state considered in Fig 1. First, QTs generates three hybrid EPR pairs at the orchestrator. Ebits at microwave and optical frequencies are depicted in blue and red respectively. After being distributed through optical channels, optical ebits of the generated EPRs are converted at microwave frequencies with a down-conversion process implemented by the QTs at the plain clients. Once the microwave EPRs are distributed between orchestrator and clients, the multipartite entangled state can be teleported to the three plain clients according to Fig 2.

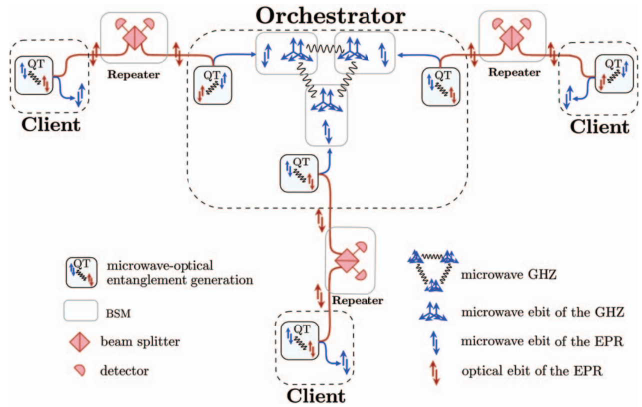


Fig. 4: TMD with complex clients: *Teleported Multipartite entanglement Distribution* with complex clients for the same multipartite state considered in Fig 1. First, QTs generates three hybrid EPR pairs at the orchestrator and one hybrid EPR pair at each client. Ebits at microwave and optical frequencies are depicted in blue and red respectively. Optical repeaters implement entanglement swapping on optical ebits of the generated EPRs (one ebit from the orchestrator and one ebit from a complex client). After the swap, the microwave EPRs are distributed between orchestrator and clients, the multipartite entangled state can be teleported to the three complex clients according to Fig 2.

## III. Quantum Transduction Models for TMD

As introduced in Sec. II, TMD strategy limits microwave-optical transduction to EPR pairs, and no quantum transduction of the multipartite ebits is performed.

Clearly, the ebit of the EPR pair to be shared can be transduced with a cascade of up- and down-conversion, as it happens in DMD strategy in Fig. 1. This choice solves one of the main two issues exhibited by DMD, namely, its unsuitability for the different classes of multipartite entanglement, characterized by different persistence properties. Furthermore, any loss or noise affect the EPR pair that, differently from the multipartite entanglement state, can be more easily regenerated. However, utilising a cascade of up- and down-conversion does not remedy to the severe inefficiency of direct quantum transduction, which requires a parameter regime for achieving not-null quantum capacity transduction still hard to reach with the state-of-the-art technology [16], [19].

Accordingly, in the following we provide two different communication models for TMD quantum transduction based on a different paradigm. This paradigm exploits the capabilities of the quantum transduction hardware to generate entanglement [23], rather than the ability of the hardware to up- or down-convert quantum states.

[2]It is worthwhile to note that the generation of the EPR pairs can happen either sequentially or in parallel, depending on the characteristics of the underlying quantum technology.

### A. QT Modelling for TMD in presence of intrinsic entanglement and "plain" clients

As mentioned above, the parameter regime for achieving not-null quantum capacity transduction between microwave and optical domains is still beyond state-of-the-art technology.

Conversely, the parameter regime achievable with state-of-the-art technology, when coupled with cryogenic temperatures so that thermal microwave noise can be neglected [24], enables the generation of *intrinsic* entanglement, i.e., entanglement between two different (optical and microwave) domains [16], [24]. Specifically, through spontaneous parametric down-conversion [3] (SPDC) of an input pump field, entanglement between optical and microwave fields is generated within the transducer [16], [26]–[28]. It is worthwhile to highlight that, similarly to up- and down-conversion, entanglement generation via SPDC within the transducer is not deterministic. Indeed, there exists the possibility that this process fails and no entanglement between microwave and optical field is generated.

In the following, we suppose that the generated bipartite entanglement is an EPR pair formed by two photons, and thus it can be expressed with *Fock* state notation as:

$$|\Phi^o_{MO}\rangle = \frac{1}{\sqrt{2}}(|0^o_M 0^o_O\rangle + |1^o_M 1^o_O\rangle). \quad (1)$$

[3]Spontaneous parametric down-conversion is a non-linear optical process where a photon spontaneously splits into two photons of lower energies [25]

with the subscripts $M$ and $O$ denoting the photon domain – i.e., microwave and optical – whereas the superscript denoting the "location" of each ebit, which is $o$ as orchestrator at the generation of the EPR. [27]. Accordingly, in (1) the term $|1^o_M 1^o_O\rangle$ denotes the event in which SPDC successfully generated a couple of photons, one at microwave and the other at optical frequency. Conversely, the term $|0^o_M 0^o_O\rangle$ denotes the event in which SPDC failed, and no microwave nor optical photon have been generated.

**Remark.** *The two assumptions underlying equation* (1) *must be better discussed. Regarding the assumption of generating a two-level state – i.e., the assumption of restricting the admissible system state to 2-level Fock states for each field rather than an uncountable levels – is not restrictive, since it simply requires a specific inizialization (aka red detuning) of the microwave field inside the cavity [27]. This leads to an EPR state in the form of* $\frac{1}{\sqrt{2}}(|01\rangle + |10\rangle)$ *as discussed in Sec. IV-B, which is equivalent to* (1) *up to a basis change. Thus, in the following we will use* (1). *Furthermore, also the assumption of an EPR state – i.e., a maximally entangled state with even superposition of two states as in* (1) *– depends on a careful setting of the transduction hardware parameters [27]. Obviously, any hardware mismatch from the ideal setting would impact on the purity of the generated entangled pair.*

Stemming from the above, we can model the TMD with intrinsic entanglement generated by the transducer at the orchestrator as in Fig. 3. Specifically, $n$ intrinsic EPR pairs are generated at the orchestrator, with the optical ebit of each EPR pair transmitted to each client and down-converted to the microwave domain therein, resulting in the following EPR state:

$$|\Phi^{oc}_{MM}\rangle = \frac{1}{\sqrt{2}}(|0^o_M 0^c_M\rangle + |1^o_M 1^c_M\rangle), \tag{2}$$

shared between the orchestrator $o$ and the arbitrary client $c \in \{1, \dots, n\}$. Accordingly, once the $n$ EPRs are distributed through the network, the overall state $|\phi_{QT_s}\rangle$ is given by:

$$|\phi_{QT_s}\rangle = |\psi_{me}\rangle \otimes |\Phi^{oc}_{MM}\rangle^{\otimes n}, \tag{3}$$

with $|\psi_{me}\rangle$ denoting the multipartite entangled state to be distributed to the $n$ clients. The teleportation of the multipartite entangled state can be now be performed.

**Remark.** *This model requires each client to be equipped with a quantum transducer capable of down-converting from optical to microwave. This represents the "simplest" form of hardware transduction at the clients – as denoted by the subscript s of* $|\phi_{QT_s}\rangle$ *in* (3) *– making so the model appealing in terms of client requirements. Yet, it suffers from the inefficiency of direct quantum transduction – although limited to a single conversion – optical to micro – rather than two conversions – micro to optical and then back to micro – as for DMD.*

### *B. QT Modelling for TMD in presence of intrinsic entanglement and "complex" clients*

An alternative model for TMD is obtained by relaxing the assumption of concentrating hardware complexity at the orchestrator. Specifically, it is obtained by assuming that clients are characterised by higher hardware capabilities – and thus they are able to generate intrinsic EPR pairs between microwave and optical domains – and additional hardware is dislocating along the optical links.

Accordingly, the generation of the EPR pairs occurs "at both points" rather than at "source only" [12], [29], as shown in Fig. 4. Specifically, $n$ intrinsic EPR pairs are generated at the orchestrator and $n$ intrinsic EPR pairs are generated at the clients. As for the first scheme, each EPR pair is hybrid, by involving both the microwave and optical domains. EPR pairs are eventually distributed between orchestrator and clients through a procedure resembling entanglement swapping [30]. This procedure accounts for the nature of the Fock states in (1) [31], and it is described in details in the following.

The Fock state at each client can be written as follows:

$$|\Phi^{c}_{MO}\rangle = \frac{1}{\sqrt{2}}(|0^c_M 0^c_O\rangle + |1^c_M 1^c_O\rangle). \tag{4}$$

and $n$ Fock states as in (1) are available at the orchestrator.

The optical ebits of each EPR are thus transmitted through optical quantum channels and reach $n$ beam splitters, one for each client, and each beam splitter is followed by two detectors, so that the overall setup is unable to distinguishing the *which-path* information [27], [31]. A click of one of the two detectors of each setup denotes the presence of an optical photon. However, due to the path-erasure, the impossibility of knowing whether the optical photon responsible for the detector-click has been generated at the orchestrator or at the client makes it impossible to distinguish where the SPDC has taken place, and thus whether a microwave photon is present at orchestrator or at client. This results into the generation of a *path-entanglement* [32] between the microwave photon at the orchestrator and at the client [27]. Thus, the overall effect of beam splitter and detectors is reminiscent of entanglement swapping, since they project the received optical photons into a Bell state and the heralded signal – i.e., the detector-click – indicates the distribution of entangled pairs in the remote superconducting processors [33]:

$$|\Psi^{oc}_{MM}\rangle = \frac{1}{\sqrt{2}}(|0^o_M 1^c_M\rangle + |1^o_M 0^c_M\rangle). \tag{5}$$

Accordingly, the overall state $|\phi_{QT_c}\rangle$, after the swapping-like distribution procedure, can be ideally expressed as:

$$|\phi_{QT_c}\rangle = |\psi_{me}\rangle \otimes |\Psi^{oc}_{MM}\rangle^{\otimes n}. \tag{6}$$

and the teleportation of the multipartite entangled state $|\psi_{me}\rangle$ do be distributed can be performed.

## IV. Noisy Transduction Models for TMD

From the discussions within the previous sections, it is clear that the challenges in TMD strategies shift from preserving the

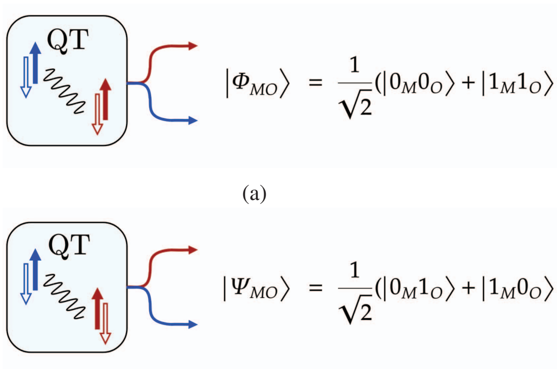


(a)

(b)

Fig. 5: Different intrinsic entanglement generation schemes (a) withouth, and (b) with inizializaton of the microwave field inside the cavity. Blue (red) "up"-solid arrows represent the presence of a microwave (optical) photon, while blue (red) "down"-empty arrows denote the absence of a microwave (optical) photon.

multipartite state during frequency up- and down conversions (and during the optical propagation) to preserving the EPR pairs that will be utilized for teleporting the multipartite state.

Hence, in this section we carried out a comparison analysis between the two models presented in Sec. III. However, this analysis is very far from being exhaustive. The reason is that the hardware influences hugely this comparison. And there is not a single hardware solution individuated in literature. Accordingly, we will provide guidelines for this comparison from a communication network perspective. And we do hope that this paper will push the hardware community to converge on a standard reference model, which would be of paramount importance for quantum network development.

Since the interest is on the QT model performance, we will neglect the noise effects on the generation process of the multipartite entangled state, by reasonably assuming that proper noise-cancellation or state-purification techniques can be adopted during the generation process within the orchestrator.

### A. *Noisy QT model for TMD in presence of plain clients*

For the model introduced in Section III-A, the purity of the EPR pairs in equation (2) is affected by the efficiency and features of the transducers available at the orchestrator as well as by the efficiency and features of the down-convertion transducer available at the clients. For abstracting from the particulars of the underlying technolgies, we capture the transducer features at the orchestrator and at the clients through the parameters $\eta_h^o$ and $\eta_{dc}^c$, respectively.

As a consequence, in practical scenarios, due to noise effects, the shared pair between the orchestrator and the arbitrary client deviated from the ideal pure state in eq. (2). And it can be modelled as a *Werner state*, whose density matrix is expressed as follows [34]:

$$\rho = p\,|\Phi_{MM}^{oc}\rangle\langle\Phi_{MM}^{oc}| + (1-p)\frac{\mathbb{I}_4}{4} \triangleq p\rho_{QT_s}^{id} + (1-p)\rho_{QT_s}^{ni} \tag{7}$$

with $\mathbb{I}_4$ denoting the identity matrix of dimension 4. The parameter $p$, which is the probability that the state is not affected by noise – i.e., the probability of obtaining the ideal state $\rho_e^{id} \triangleq |\Phi_{MM}^{oc}\rangle\langle\Phi_{MM}^{oc}|$ – is a function, $f(\cdot)$, of the transducer parameters $\eta_h^o$ and $\eta_{dc}^c$, as well as of the features $\eta_{qc}$ of the considered quantum channel:

$$p \sim f(\eta_h^o, \eta_{dc}^c, \eta_{qc}). \tag{8}$$

It is worthwhile to note that modeling the shared state as a Werner state corresponds to the worst-case scenario [35].

Stemming from this, the state of the overall system cannot be anymore expressed as in equation (3), since the noise induced on the overall state a non-unitary evolution. To express the state of the overall system through a closed-form expression, we need to consider all the error configurations affecting the different distribution processes.

To this aim, it is convenient to describe the error configurations on the $n$ links between the orchestrator and the clients through binary sequences of length $n$, where "0" in the position $j$ denotes that on the j-th link no-error occurred, whereas "1" in the position $j$ denotes that on the j-th link the error occurred. The set $S$ of the aforementioned binary sequences has a cardinality $|S|$ given by:

$$|S| = \sum_{k=0}^{n}\binom{n}{k} = 2^n, \tag{9}$$

where $\binom{n}{k}$ denotes the binomial coefficient representing the number of binary sequences in $S$ characterized by $k$ links among $n$ in error. The subset $S^{(k)} \subset S$ of $S$ constituted by sequences with $k$ ones has thus cardinality $|S^{(k)}| = \binom{n}{k}$. In the following, we denote with $S_i$ the i-th binary sequence in $S$ and with $S_{ij}$ the j-th elemnt of $S_i$. Stemming from this, and by accounting for (7), it results that:

$$\rho_{QT_S}^{S_{ij}} = \begin{cases} \rho_{QT_s}^{id}, & \text{if } S_{ij} = 0, \\ \rho_{QT_s}^{ni}, & \text{otherwise.} \end{cases} \tag{10}$$

By using (10), the state of the overall system can be expressed as:

$$\rho_{QT_s} = \rho_{me} \otimes \left( \sum_{i=1}^{|S|} \otimes_{j=1}^{n} p_{S_{ij}}\, \rho_{QT_S}^{S_{ij}} \right) = \\ = \rho_{me} \otimes \Bigg( p^n (\rho_{QT_s}^{id})^{\otimes n} + (1-p)^n (\rho_{QT_s}^{ni})^{\otimes n} + \\ + \sum_{k=1}^{n-1} \sum_{i:S_i \in S^{(k)}} p^{n-k}(1-p)^k \left( \otimes_{j=1}^{n} \rho_{QT_S}^{S_{ij}} \right) \Bigg). \tag{11}$$

If entanglement purification is performed, a recurrence of local operations [36], [37] have to be applied for each Werner state (7). The number of iterations depends on the targeted fidelity, as well as on the transducer parameters, which, in turn, affect also the initial fidelity of the generated state.

### *B. Noisy QT model for TMD in more complex clients*

For the model introduced in Section III-B, the purity of the EPR pairs in equation (5) is affected by the efficiency and features of the transducers available at the orchestrator and at the clients – which can be reasonable assumed as of the same type – as well as by the efficiency and features of the beamsplitters and detectors.

Here, we capture the features of the transducer at the orchestrator and at the clients through the parameters $\eta_n^o$ and $\eta_n^c$. And, we embrace the features of beamsplitters and detectors, by introducing the parameter $\eta_s$.

As described in Sec. III-B, this model requires the detection of a single optical photon. However, it may happen that two optical photons travel along the quantum channel connecting orchestrator with client and reach the beam-splitter, since the entanglement generation can be successfull at both sides. Due to path erasure, only one detector click is triggered. In such a case, a detector click corresponds to the presence of two microwave photons, one at the orchestrator and one at the client [33]. Thus the state shared between the orchestrator and the client is not the ideal entangled state in (5), and it can be expressed as:

$$\rho = q \overbrace{|\Psi_{MM}^{oc}\rangle \langle \Psi_{MM}^{oc}|}^{\triangleq \rho_{QT_c}^{id}} + (1-q) \overbrace{|1_M^o 1_M^c\rangle \langle 1_M^o 1_M^c|}^{\triangleq \rho_{QT_c}^{ni}}. \qquad (12)$$

The parameter $q$, which is the probability that the state is not affected by noise – i.e. the ideal state $|\Psi_{MM}^{oc}\rangle \langle \Psi_{MM}^{oc}|$ is obtained – is a function, $g(\cdot)$, of the transducer parameters $\eta_h^o$ and $\eta_h^c$, as well as of the features $\eta_s$ of beamsplitters and detectors and of the considered quantum channel:

$$q \sim g(\eta_h^o, \eta_h^c, \eta_s, \eta_{qc}). \qquad (13)$$

Stemming from this, the state of the overall system cannot be anymore expressed as in equation (6). By adopting a similar reasoning as for the previous model, and by accounting for (12), it results:

$$\rho_{QT_c}^{S_{ij}} = \begin{cases} \rho_{QT_c}^{id}, & \text{if } S_{ij} = 0, \\ \rho_{QT_c}^{ni}, & \text{otherwise.} \end{cases} \qquad (14)$$

Thus, the state of the overall system is given as follows:

$$\rho_{QT_c} = \rho_{me} \otimes \Bigg( q^n (\rho_{QT_c}^{id})^{\otimes n} + (1-q)^n (\rho_{QT_c}^{ni})^{\otimes n} + \sum_{k=1}^{n-1} \sum_{i:S_i \in S^{(k)}} q^{n-k} (1-q)^k \left( \otimes_{j=1}^n \rho_{QT_c}^{S_{ij}} \right) \Bigg). \qquad (15)$$

For this QT model, differently from the first model, if entanglement purification is performed, one can apply directly bilateral local CNOT operations [36], followed by measurements in the computational basis on the target qubits involved in the CNOT operations. And we stress that the CNOT operations are local since they involve the qubits of the mixed states at the orchestrator and at the client. Indeed, if the measurement returns the state $|11\rangle$, the state collapses in $|\Psi_{MM}^{oc}\rangle$ with fidelity 1.

### *C. Discussion*

As described in Sec. III-B, the complex-client model requires the detection of a single optical photon. However, it may happen that the SPDC processes at the orchestrator and at the client are successful. So two optical photons travel along the quantum channel connecting the orchestrator and the client and reach the beam-splitter. But due to path erasure, only one detector click is triggered. In such a case, a detector click corresponds to the presence of two microwave photons, one at the orchestrator and one at the client. Thus the state shared between the orchestrator and the client is $|1_M^o\rangle |1_M^c\rangle$ and it is not the entangled state[4] in (5).

In the $QT_c$ model, the sources of noise are not limited to the above case. Indeed, it is possible that multiple photons are generated at both the orchestrator and at the client. This event happens with no-null probabilities [27], [38] depending on the hardware features through the parameters $\eta_h^o$ and $\eta_h^c$. In other words, Fock states $|n_O^o m_O^c\rangle$ with $n_O^o$ optical photons at the orchestrator and $m_O^c$ optical photons at the client have to be considered.

While the first noise source – i.e. SPDC processes at the orchestrator and at the client both successful – is unavoidable, the second one – i.e. Fock states $|n_O^o m_O^c\rangle$ – can be removed either by utilizing single-photon counter detectors or with a proper inizialization (aka red detuning) of the microwave field inside the cavity as discussed in the Remark after equation (1) and shown in Fig. 5. Indeed, with the setup shown in Fig. 5b, it is not possible to generate more the one optical photon for each involved node. Therefore, the entanglement purity is only affected by the possibility that both microwave photon (at the orchestrator and client) are up-converted.

## V. Conclusion

In this paper we presented two different communication models for multipartite entanglement distribution based on recent advances in quantum transduction devices to go beyond direct conversion. And we move a step forward towards a comparison analysis between the two models. However, this analysis is very far from being exhaustive. The reason is that the hardware influences hugely this comparison. And there is not a single hardware solution individuated in literature. Accordingly, we provided guidelines for this comparison from a communication network perspective. And we do hope that this paper will push the hardware community to converge on a standard reference model, which would be of paramount importance for quantum network development.

[4]We observe that when the SPDC processes at the orchestrator and at the client both fail, i.e., no optical photon is generated, there is no click of the detectors. Thus, this event does not affect the purity of the generated entanglement.

## References


[1] A. S. Cacciapuoti, M. Caleffi, F. Tafuri, F. S. Cataliotti, S. Gherardini, and G. Bianchi, "Quantum internet: Networking challenges in distributed quantum computing," IEEE Network, vol. 34, no. 1, pp. 137–143, 2020.

[2] J.-G. Ren, P. Xu, H.-L. Yong, L. Zhang, S.-K. Liao, J. Yin, W.-Y. Liu, W.-Q. Cai, M. Yang, L. Li et al., "Ground-to-satellite quantum teleportation," Nature, vol. 549, no. 7670, pp. 70–73, 2017.

[3] M. Caleffi, A. S. Cacciapuoti, and G. Bianchi, "Quantum internet: From communication to distributed computing!" in Proceedings of the 5th ACM international conference on nanoscale computing and communication, 2018, pp. 1–4.

[4] N. Lauk, N. Sinclair, S. Barzanjeh, J. Covey, M. Saffman, M. Spiropulu, and C. Simon, "Perspectives on quantum transduction," Quantum Science and Technology, vol. 5, 02 2020.

[5] F. S. Nicholas J. Lambert, Alfredo Rueda and H. G. L. Schwefel, "Coherent conversion between microwave and optical photons—an overview of physical implementations," Advanced Quantum Technologies (Online), vol. 3, 2020.

[6] A. Rueda, F. Sedlmeir, M. C. Collodo, U. Vogl, B. Stiller, G. Schunk, D. V. Strekalov, C. Marquardt, J. M. Fink, O. Painter, G. Leuchs, and H. G. L. Schwefel, "Efficient microwave to optical photon conversion: an electro-optical realization," Optica, vol. 3, no. 6, pp. 597–604, Jun 2016. [Online]. Available: https://opg.optica.org/optica/abstract.cfm?URI=optica-3-6-597

[7] W. Hease, A. Rueda, R. Sahu, M. Wulf, G. Arnold, H. G. Schwefel, and J. M. Fink, "Bidirectional electro-optic wavelength conversion in the quantum ground state," PRX Quantum, vol. 1, p. 020315, Nov 2020. [Online]. Available: https://link.aps.org/doi/10.1103/PRXQuantum.1.020315

[8] W. Dür, G. Vidal, and J. I. Cirac, "Three qubits can be entangled in two inequivalent ways," Phys. Rev. A, vol. 62, p. 062314, Nov 2000. [Online]. Available: https://link.aps.org/doi/10.1103/PhysRevA.62.062314

[9] J. Illiano, M. Caleffi, A. Manzalini, and A. S. Cacciapuoti, "Quantum internet protocol stack: A comprehensive survey," Computer Networks, p. 109092, 2022.

[10] A. S. Cacciapuoti, M. Viscardi, J. Illiano, and M. Caleffi, "Entanglement distribution in the quantum internet: Knowing when to stop!" 07 2023.

[11] J. Illiano, M. Caleffi, M. Viscardi, and A. S. Cacciapuoti, "Quantum mac: Genuine entanglement access control via many-body dicke states," IEEE Transactions on Communications, vol. PP, pp. 1–1, 01 2023.

[12] A. S. Cacciapuoti, M. Caleffi, R. Van Meter, and L. Hanzo, "When entanglement meets classical communications: Quantum teleportation for the quantum internet," IEEE Transactions on Communications, vol. 68, no. 6, pp. 3808–3833, 2020.

[13] D. M. Greenberger, M. A. Horne, A. Shimony, and A. Zeilinger, "Bell's theorem without inequalities," American Journal of Physics, vol. 58, no. 12, pp. 1131–1143, 1990.

[14] R. Eleanor and P. Wolfgang, Quantum Computing: A Gentle Introduction, 1st ed. The MIT Press, 2011.

[15] J. Holzgrafe, N. Sinclair, D. Zhu, A. Shams-Ansari, M. Colangelo, Y. Hu, M. Zhang, K. K. Berggren, and M. Lončar, "Cavity electro-optics in thin-film lithium niobate for efficient microwave-to-optical transduction," Optica, vol. 7, no. 12, pp. 1714–1720, Dec 2020. [Online]. Available: https://opg.optica.org/optica/abstract.cfm?URI=optica-7-12-1714

[16] J. Wu, C. Cui, L. Fan, and Q. Zhuang, "Deterministic microwave-optical transduction based on quantum teleportation," Phys. Rev. Appl., vol. 16, p. 064044, Dec 2021. [Online]. Available: https://link.aps.org/doi/10.1103/PhysRevApplied.16.064044

[17] M. Tsang, "Cavity quantum electro-optics. ii. input-output relations between traveling optical and microwave fields," Physical Review A, vol. 84, no. 4, p. 043845, 2011.

[18] L. Fan, C.-L. Zou, R. Cheng, X. Guo, X. Han, Z. Gong, S. Wang, and H. X. Tang, "Superconducting cavity electro-optics: a platform for coherent photon conversion between superconducting and photonic circuits," Science advances, vol. 4, no. 8, p. eaar4994, 2018.

[19] C. Zhong, X. Han, and L. Jiang, "Microwave and optical entanglement for quantum transduction with electro-optomechanics," Phys. Rev. Appl., vol. 18, p. 054061, Nov 2022. [Online]. Available: https://link.aps.org/doi/10.1103/PhysRevApplied.18.054061

[20] A. S. Cacciapuoti, J. Illiano, M. Viscardi, and M. Caleffi, "Entanglement distribution in the quantum internet: Knowing when to stop!" 2024.

[21] H. Zhou, T. Li, and K. Xia, "Parallel and heralded multiqubit entanglement generation for quantum networks," Phys. Rev. A, vol. 107, p. 022428, Feb 2023. [Online]. Available: https://link.aps.org/doi/10.1103/PhysRevA.107.022428

[22] G. Avis, F. Rozpedek, and S. Wehner, "Analysis of multipartite entanglement distribution using a central quantum-network node," Phys. Rev. A, vol. 107, p. 012609, Jan 2023. [Online]. Available: https://link.aps.org/doi/10.1103/PhysRevA.107.012609

[23] A. Kyle, C. L. Rau, W. D. Warfield, A. Kwiatkowski, J. D. Teufel, K. W. Lehnert, and T. Dennis, "Optically distributing remote two-node microwave entanglement using doubly parametric quantum transducers," Phys. Rev. Appl., vol. 20, p. 014005, Jul 2023. [Online]. Available: https://link.aps.org/doi/10.1103/PhysRevApplied.20.014005

[24] M. Tsang, "Cavity quantum electro-optics. ii. input-output relations between traveling optical and microwave fields," Phys. Rev. A, vol. 84, p. 043845, Oct 2011. [Online]. Available: https://link.aps.org/doi/10.1103/PhysRevA.84.043845

[25] C. Couteau, "Spontaneous parametric down-conversion," Contemporary Physics, vol. 59, no. 3, pp. 291–304, 2018.

[26] A. Rueda, W. Hease, S. Barzanjeh, and J. Fink, "Electro-optic entanglement source for microwave to telecom quantum state transfer," 09 2019.

[27] S. Krastanov, H. Raniwala, J. Holzgrafe, K. Jacobs, M. Lončar, M. J. Reagor, and D. R. Englund, "Optically heralded entanglement of superconducting systems in quantum networks," Phys. Rev. Lett., vol. 127, p. 040503, Jul 2021. [Online]. Available: https://link.aps.org/doi/10.1103/PhysRevLett.127.040503

[28] C. Zhong, Z. Wang, C. Zou, M. Zhang, X. Han, W. Fu, M. Xu, S. Shankar, M. H. Devoret, H. X. Tang, and L. Jiang, "Proposal for heralded generation and detection of entangled microwave–optical-photon pairs," Physical Review Letters, vol. 124, no. 1, Jan. 2020. [Online]. Available: http://dx.doi.org/10.1103/PhysRevLett.124.010511

[29] W. Kozlowski, S. Wehner, R. V. Meter, B. Rijsman, A. S. Cacciapuoti, M. Caleffi, and S. Nagayama, "Architectural Principles for a Quantum Internet," RFC 9340, Mar. 2023.

[30] H.-J. Briegel, W. Dür, J. I. Cirac, and P. Zoller, "Quantum repeaters: The role of imperfect local operations in quantum communication," Phys. Rev. Lett., vol. 81, pp. 5932–5935, Dec 1998. [Online]. Available: https://link.aps.org/doi/10.1103/PhysRevLett.81.5932

[31] R. Pakniat, M. H. Zandi, and M. K. Tavassoly, "On the entanglement swapping by using the beam splitter," European Physical Journal Plus, vol. 132, no. 1, p. 3, Jan. 2017.

[32] F. Monteiro, V. C. Vivoli, T. Guerreiro, A. Martin, J.-D. Bancal, H. Zbinden, R. T. Thew, and N. Sangouard, "Revealing genuine optical-path entanglement," Phys. Rev. Lett., vol. 114, p. 170504, May 2015. [Online]. Available: https://link.aps.org/doi/10.1103/PhysRevLett.114.170504

[33] L. Duan, M. Lukin, J. Cirac, and P. Zoller, "Long-distance quantum communication with atomic ensembles and linear optics," Nature, vol. 414, pp. 413–8, 12 2001.

[34] R. F. Werner, "Quantum states with einstein-podolsky-rosen correlations admitting a hidden-variable model," Phys. Rev. A, vol. 40, pp. 4277–4281, Oct 1989. [Online]. Available: https://link.aps.org/doi/10.1103/PhysRevA.40.4277

[35] K. Chakraborty, D. Elkouss, B. Rijsman, and S. Wehner, "Entanglement distribution in a quantum network: A multicommodity flow-based approach," IEEE Transactions on Quantum Engineering, vol. 1, pp. 1–21, 2020.

[36] C. H. Bennett, D. P. DiVincenzo, J. A. Smolin, and W. K. Wootters, "Mixed-state entanglement and quantum error correction," Physical Review A, vol. 54, no. 5, p. 3824–3851, Nov. 1996. [Online]. Available: http://dx.doi.org/10.1103/PhysRevA.54.3824

[37] C. H. Bennett, G. Brassard, S. Popescu, B. Schumacher, J. A. Smolin, and W. K. Wootters, "Purification of noisy entanglement and faithful teleportation via noisy channels," Physical Review Letters, vol. 76, no. 5, p. 722–725, Jan. 1996. [Online]. Available: http://dx.doi.org/10.1103/PhysRevLett.76.722

[38] L. d'Avossa, M. Caleffi, C. Wang, J. Illiano, S. Zorzetti, and A. S. Cacciapuoti, "Towards the quantum internet: entanglement rate analysis of high-efficiency electro-optic transducer." [Online]. Available: https://www.osti.gov/biblio/2006497